

Metasurface inverse designed by deep learning for quasi-entire terahertz wave absorption: supporting information

Zhipeng Ding^a, Wei Su^{a}, Yinlong Luo^a, Lipengan Ye^a, Wenlong Li^a, Yuanhang Zhou^a, Jianfei Zou^a, Bin Tang^b, and Hongbing Yao^{a**}*

^aHohai University, College of Science, 211100, Nanjing, China

^bSchool of Microelectronics and Control Engineering, Changzhou University, Changzhou 213164, China

*E-mail: opticsu@hhu.edu.cn.

**E-mail: alenyao@hhu.edu.cn.

1. Simulation setup

In this study, the absorption characteristics of UTWMA were investigated using the finite-difference time-domain (FDTD) method, employing periodic boundary conditions in both x - and y -directions, and a perfectly matched layer (PML) is set in the z -direction for numerical solution. The wave source is set to plane wave. The incident wave frequency was set within the range of 0.1 - 10 THz, and the mesh accuracy was set to 6, with additional mesh layers added to all GLs to ensure the simulation accuracy. The incident wave was incident vertically along the negative z -axis, and two monitors were added above the light source and at the bottom of the UTWMA to obtain the reflection $R(\omega)$ and transmission $T(\omega)$, and the absorption $A(\omega)$ can be obtained according to $A(\omega) = 1 - R(\omega) - T(\omega)$. As the Ag layer effectively prevented the downward transmission of the THz wave, the transmitted wave was considered to converge to 0, simplifying the absorption expression further to $A(\omega) = 1 - R(\omega)$.

2. Table S1

Table S1. The range and minimum accuracy of structural parameters of UTWMA.

Parameter	Range (μm)	Minimum accuracy (μm)
d_1	5.0 ~ 40.0	0.1 μm
d_2	8.0 ~ 45.0	0.1 μm
d_3	10.0 ~ 55.0	0.1 μm
h_1	5.0 ~ 50.0	0.1 μm
h_2	1.0 ~ 20.0	0.1 μm
h_3	1.0 ~ 20.0	0.1 μm
h_4	1.0 ~ 20.0	0.1 μm
h_5	0.5	-

3. Fig. S1

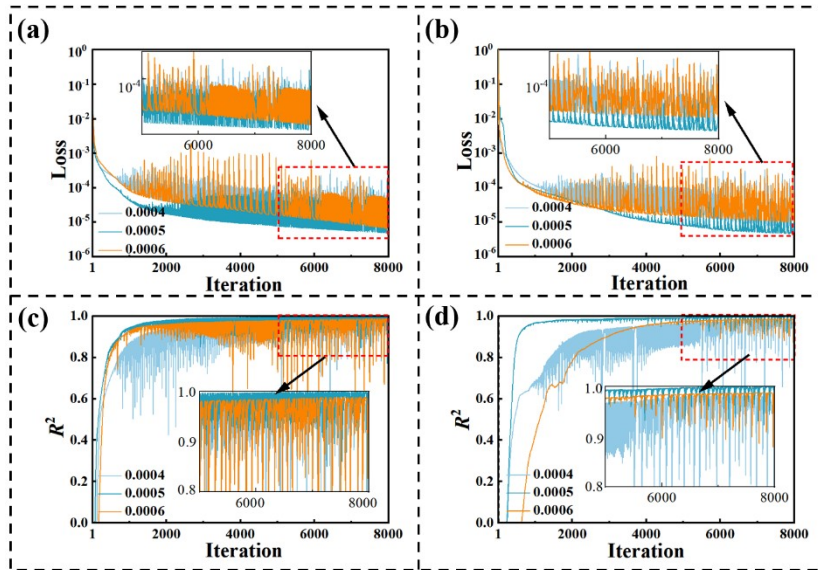


Fig. S1. Loss function and R^2 for the training and test sets with different LR based on ANN training. (a-b) Loss function for the training and test sets. (c-d) R^2 for the training and test sets.

4. Fig. S2

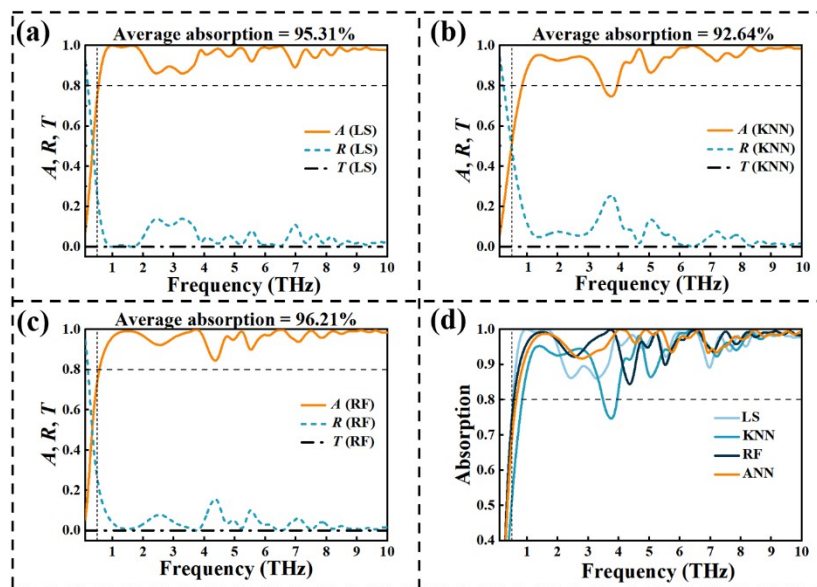


Fig. S2. Absorption $A(\lambda)$, reflection $R(\lambda)$, and transmission $T(\lambda)$ spectra obtained by inverse design of different algorithm models and comparison of absorption spectra. (a-c) Absorption $A(\lambda)$, reflection $R(\lambda)$, and transmission $T(\lambda)$ spectra obtained by LS, KNN, and RF inverse design. (d) Comparison of absorption spectra obtained by inverse design of different algorithm models.

5. Table S2

Table S2. Geometric parameters and the predicted average absorptivity of the inverse design output of different algorithmic models

Types of algorithms	LS	KNN	RF	ANN
d_1 (μm)	19.5	13.1	13.0	10.9
d_2 (μm)	49.0	44.7	43.9	44.1
d_3 (μm)	48.7	49.1	43.9	44.1
h_1 (μm)	49.0	48.2	49.9	49.1
h_2 (μm)	8.1	7.9	7.9	8.0
h_3 (μm)	6.9	13.5	13.6	13.5
h_4 (μm)	22.1	8.9	14.4	11.5
Predicted average absorptivity	97.51%	96.08%	96.04%	96.31%
True average absorptivity	95.31%	92.64%	96.21%	96.33%

6. Supplementary formula

$$MAPE = \frac{1}{n} \sum_{i=1}^n \left| \frac{y_i - \hat{y}_i}{y_i} \right| \times 100\%$$

*

MERGEFORMAT (4)

$$RMSE = \sqrt{\frac{\sum_{i=1}^n (y_i - \hat{y}_i)^2}{n}}$$

*

MERGEFORMAT (5)

where y_i and \hat{y}_i represent the true and predicted values of the average absorptivity of the UTWMA test set, respectively.

7. Fig. S3

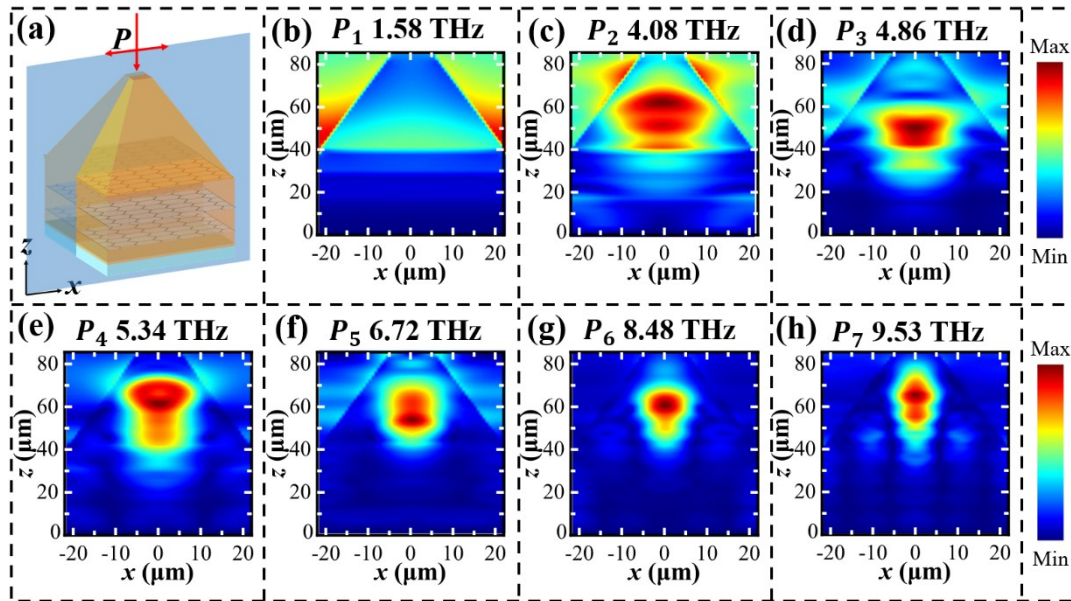


Fig. S3. Analysis of the absorbed power of the UTWMA. (a) Schematic representation of the absorbed power along the x - z plane under normal TE-polarization incident THz wave. (b-h) The absorbed power along the x - z plane under normal TE-polarization incident THz wave at P_1 , P_2 , P_3 , P_4 , P_5 , P_6 , and P_7 .